

## Effect of local web buckling on the cyclic behavior of reduced web beam sections (RWBS)

Vahid Akrami<sup>a</sup> and Saeed Erfani<sup>\*</sup>

Civil Engineering Department, Amirkabir University of Technology, Tehran, Iran

(Received July 30, 2014, Revised September 03, 2014, Accepted September 05, 2014)

**Abstract.** Application of reduced web beam section (RWBS) as a sacrificial fuse element has become a popular research field in recent years. Weakening of beam web in these connections may cause local web buckling around the opening area which can affect cyclic behavior of connection including: maximum load carrying capacity, strength degradation rate, dissipated energy, rotation capacity, etc. In this research, effect of local web buckling on the cyclic behavior of RWBS connections is investigated using finite element modeling (FEM). For this purpose, a T-shaped moment connection which has been tested under cyclic loading by another author is used as the reference model. Fracture initiation in models is simulated using Cyclic Void Growth Model (CVGM) which is based on micro-void growth and coalescence. Included in the results are: effect of opening corner radii, opening dimensions, beam web thickness and opening reinforcement. Based on the results, local web buckling around the opening area plays a significant role on the cyclic behavior of connection and hence any parameter affecting the local web buckling will affect entire connection behavior.

**Keywords:** moment resisting frames; reduced web beam section; cyclic loading; local web buckling

### 1. Introduction

According to previous research (Yang *et al.* 2009, Hedayat and Celikag 2009, Erfani *et al.* 2012), opening in beam web short away clear of beam-to-column connection is an effective method to improve the aseismic behaviors of steel moment resisting frames (MRFs). A large amount of research efforts on the structural behaviour of steel beams with web opening have been reported in the literature. Most of the early researches focused on the preparation of design recommendations for perforated beams (Redwood 1993, Darwin 2000). Later studies concerned with beneficial effects of reduced web beam sections (RWBS) under monotonic and cyclic loadings. Chung *et al.* (2001) conducted a numerical study to investigate Vierendeel mechanism in steel beams with circular web openings. In another work, Liu and Chung (2003) studied beams with web openings of various shapes and derived empirical moment–shear interaction curves. Lepage *et al.* (2004) used the reduced web section beams in the lateral resisting system. Kazemi and Erfani (2007) modeled reduced web sections using a mixed shear-flexural hinge element and concluded that the existence of opening in beam web can improve the seismic behaviour of

<sup>\*</sup>Corresponding author, Assistant Professor, E-mail: [sderfani@aut.ac.ir](mailto:sderfani@aut.ac.ir)

<sup>a</sup> Ph.D. Student, E-mail: [v.akrami@aut.ac.ir](mailto:v.akrami@aut.ac.ir)

moment frames by bringing the location of plastic hinge from the end connections to the interior parts of the beam. Tsavdaridis and D'Mello (2012) optimized beams with elliptical web openings and showed that perforations with 3:4 width to depth ratio will behave more effectively. Kazemi *et al.* (2012) studied moment connections with rectangular web openings under monotonic loading and derived a moment-shear interaction formula for design purposes. In addition to numerical studies, the feasibility of beam-to-column connections with web opening has been evaluated experimentally by some researchers. Lee *et al.* (2004) used results of cyclic tests on perforated cantilever beams to predict strength loss due to flange and web local buckling. Yang *et al.* (2009) have demonstrated that the presence of web openings at two ends of a beam will help to the formation of localized plastic hinges in these reduced sections, preventing the connection from entering to the region of plastic rotations.

From the theoretical point of view, brittle fracture at connection welds can be avoided by formation of Vierendeel mechanism in the weakened area; but a full consideration should be given to the real behaviour of these members, since the existence of secondary bending moment and axial forces at the weakened area may induce web buckling phenomena. In this research, effect of local web buckling on the cyclic behavior of RWBS connections is investigated using finite element modeling (FEM). Numerical models consist of T-shaped moment connections with square and rectangular web openings of different corner radii. The global behavior of numerical model is verified using the experimental results from other study. Fracture initiation in models is simulated using Cyclic Void Growth Model (CVGM). According to this model, fracture under cyclic loading is predicted to occur when the size of existing microvoids exceed the critical value. Included in the results are: effect of opening corner radii, opening dimensions, beam web thickness and opening perimeter stiffeners. The parameters, assumptions, modeling techniques and obtained results are discussed in the following sections.

## 2. Modeling and assumptions

The reference model used in this study includes a T-shaped moment connection which has been tested under cyclic loading by Shinde *et al.* (2003). This allows the global behaviour of finite element models to be verified by existing experimental data. The connection assembly consists of the half beam span and half the column height on each side of the beam. Cantilevered beam length (half the span width) is equal to 2.4 m where the full column height is 3.0 m. For all numerical models, the distance between the nearest point of the opening and the column edge is assumed to be equal to the depth of beam (i.e., 50 cm). Fig. 1(a) displays reference model along with a typical web opening. In this figure,  $a$  is the opening length,  $h$  is the opening height and  $r$  is the opening corner radii (OCR). As it will be helpful to use these parameters in dimensionless form, they are nondimensionalized as  $\beta = a / H$ ,  $\gamma = h / H$  and  $\lambda = 2r / h$ , where  $H$  is the total beam depth.

Load history recommended in AISC 341 (2010) is utilized for cyclic analyses. According to this reference, qualifying cyclic behaviour of beam-to-column moment connections shall be conducted by controlling the drift angle imposed on the connection subassembly (see Fig. 1(b)). Since the analyses conducted in this research are at connection level, effect of gravity load is not considered in the analyses. However, the gravity loads may have an important role on the behaviour of these systems which its evaluation requires more studies on models of frame level.

Non-linear material properties and large displacement effects are considered in the analyses. Material plasticity is based on a von Mises yield surface and an associated flow rule. Plastic

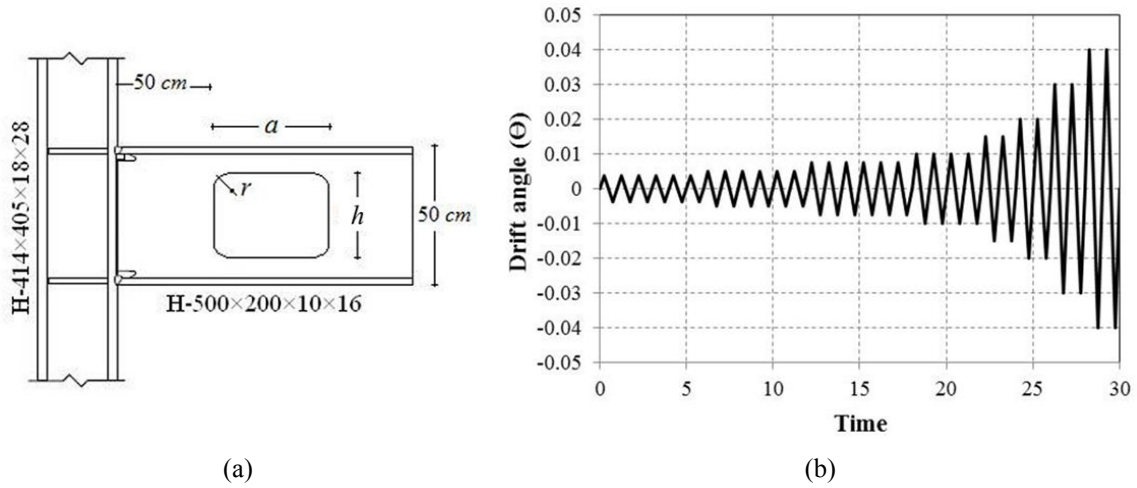


Fig. 1 Reference model and loading protocol: (a) properties of reference model; (b) loading protocol

Table 1 Mechanical properties of base metal and weld metal

Material	$E$ (GPa)	$\nu$	$\sigma_y$ (MPa)	$\sigma_u$ (MPa)	$\epsilon_u$	$\eta_{monotonic}$	$k$
Base metal	206	0.3	359.9	646.6	0.2	2.5	0.15
Weld metal	206	0.3	391.4	615.8	0.2	2.63	0.15

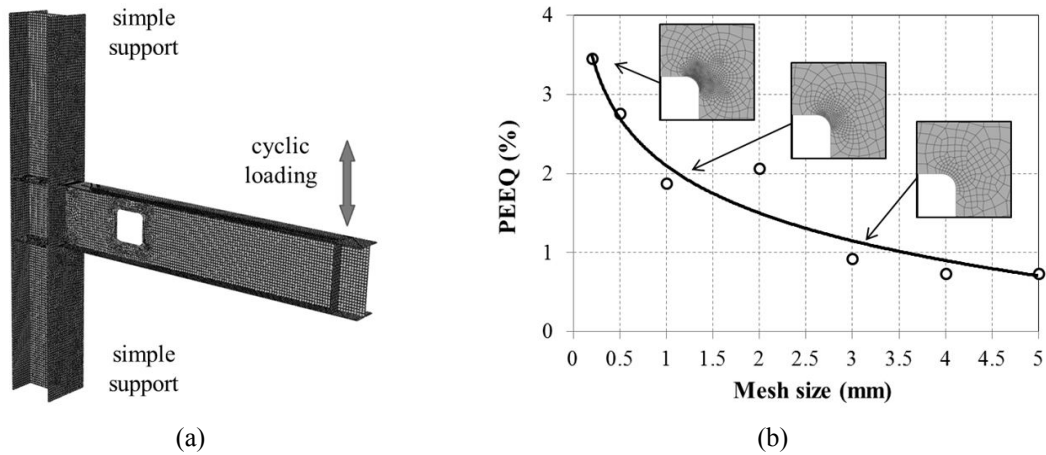


Fig. 2 Finite element modelling: (a) a numerical model of RWBS; (b) mesh sensitivity analysis

hardening is defined using combined isotropic-kinematic hardening as used by Zhou *et al.* (2012). Mechanical properties of base metal and weld metal are as listed in Table 1.

Three dimensional finite element models of the RWBS connections are established using a general purpose finite element program. The meshes consist of 4-node planar elements. Each element is separated into five layers across the thickness. A detailed global and local mesh refinement studies are performed to determine the appropriate level of mesh size for different parts

of the model. Fig. 2 displays a typical Finite element model of RWBS connection and results of sensitivity analysis in terms of equivalent plastic strain (PEEQ), for opening corners. Considering the computational expense of cyclic loading a global mesh size of  $20 \text{ mm} \times 20 \text{ mm}$  is found to be suitable for those parts of the beam and column where severe plastic deformations are not expected. For locations with steep strain gradient mesh size is limited to  $0.2 \text{ mm} \times 0.2 \text{ mm}$  which is equal to the characteristic length,  $l^*$ , required by CVGM (Kanvinde and Deierlein 2004). In order to take local and lateral buckling into account the imperfect model is used in the analyses which can be obtained by perturbing the original perfect geometry of the model using the buckling mode shapes computed in a separate buckling analysis (Hedayat and Celikag 2009).

To evaluate the modeling techniques used in this study, the reference model is subjected to cyclic loading and results are compared with the full-scale test performed by Shinde *et al.* (2003). Comparisons of hysteretic behaviors of the connections between finite element analyses and experimental tests are shown in Fig. 3. As it can be seen from this figure, the predicted load-displacement curve and buckling shape of the connection coincide well with the test results.

### 3. Characteristics of cyclic behaviour

#### 3.1 Parameters of idealized backbone curve

The backbone curve confines the hysteresis loops, defining the ultimate load resisting capacity of the system at different levels of drift. Typically, the backbone curve should at least consist of “elastic” linear part, “strain hardening” curve (characterized by decreasing but always positive stiffness) and “decaying” curve (with negative stiffness). Parameters defining the idealized backbone curve can be very useful for interpreting and evaluating the results of numerical analyses.

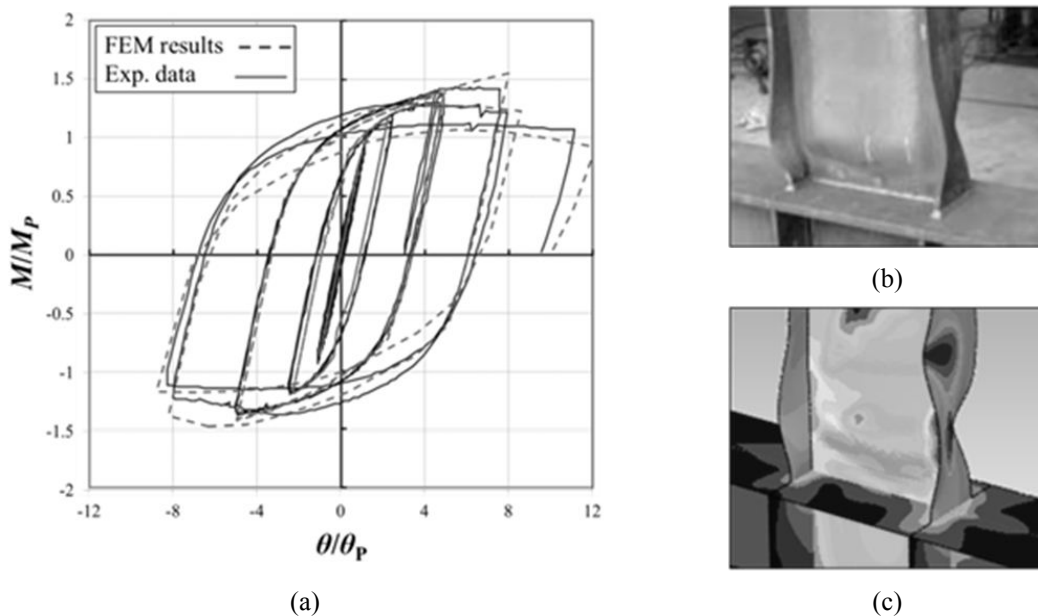


Fig. 3 Comparison of results from FEM and laboratory test

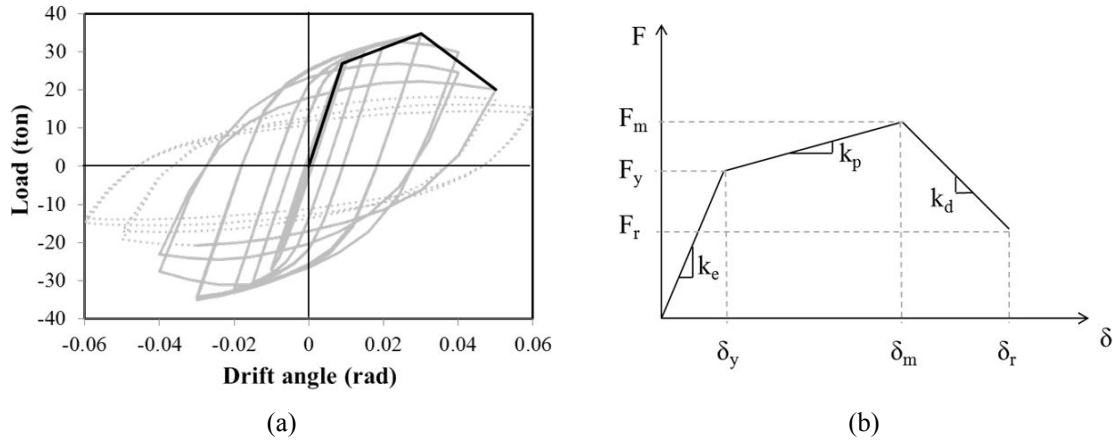


Fig. 4 Idealized backbone curve: (a) extraction of backbone curve from hysteresis curve; (b) parameters of backbone curve

analyses. Fig. 4(a) displays cyclic load-displacement curve of a RWBS connection containing an elongated circular void with  $\beta = 0.7$  and  $\gamma = 0.5$  (see Fig. 7). As it can be seen in the figure, cyclic behaviour of this model can be idealized using a trilinear backbone curve consisting of a linear portion, a strain-hardening region (which is the sign of yielding at the ends of top and bottom tee-sections) and a deterioration segment (which is mainly caused by local web buckling of the beam near the opening zone).

The main parameters defining a trilinear backbone curve include: effective yield strength and deformation ( $F_y$  and  $\delta_y$ ), effective elastic stiffness,  $K_e = F_y / \delta_y$ , maximum strength and associated deformation ( $F_m$  and  $\delta_m$ ), effective post-yield stiffness,  $K_p = (F_m - F_y) / (\delta_m - \delta_y)$ , residual strength and deformation, ( $F_r$ , and  $\delta_r$ ) and effective degrading stiffness,  $K_d = (F_m - F_r) / (\delta_r - \delta_m)$ . These parameters can be used to define a parametric backbone curve, such as the one shown in Fig. 4(b).

### 3.2 Dissipated energy

The dissipated energy is a promising parameter for characterization of structural behaviour, since it provides a consistent indication of the specimen's fatigue life, viscous damping and ductility ratio. Calculation of cumulative dissipated energy needs an appropriated failure criterion to indicate the onset of failure at numerical models. For this purpose, Cyclic Void Growth Model (CVGM) is used to model failure of specimens under Ultra-Low Cycle Fatigue (ULCF) which differ from the well-defined high cycle (more than  $10^4$  cycles) and low cycle (between  $10^2$  to  $10^4$  cycles) fatigue conditions (Myers *et al.* 2009). This model is based on the previous researches of Rice and Tracey (1969), Hancock and Mackenzie (1976) and Kanvinde *et al.* (2004). CVGM operates at the continuum-level and captures the fundamental mechanisms responsible for ductile fracture of steel structures under large inelastic strain amplitudes (several times of the yield strain) and extremely few cycles which is the case in seismic loading of MRFs. According to CVGM, ductile fracture initiation resulting from void growth and coalescence is related to the plastic strain and stress triaxiality surrounding the void. Using this approach, stress and strain histories that trigger fracture during earthquake loading can be directly modeled. According to this model, fracture under cyclic loading is predicted to occur when the cyclic fracture index  $FI_{cyclic} > 1.0$ ,

defined as

$$FI_{cyclic} = \frac{VGD_{cyclic}}{\eta_{cyclic}} \quad (1)$$

Where,  $VGD_{cyclic}$  and  $\eta_{cyclic}$  are the cyclic micro-void growth demand and capacity, respectively

$$VGD_{cyclic} = \sum_{tensile} \int_{\varepsilon_1}^{\varepsilon_2} \exp(1.5T) d\varepsilon_p - \sum_{compressive} \int_{\varepsilon_1}^{\varepsilon_2} \exp(1.5T) d\varepsilon_p \geq 0 \quad (2)$$

$$\eta_{cyclic} = \exp(-k\varepsilon_c) \cdot \eta_{monotonic} \quad (3)$$

In above equations,  $T$  is the stress triaxiality ( $T = \sigma_m / \sigma_e$ ),  $\sigma_m$  is the mean stress,  $\sigma_e$  is the effective stress (von-Mises stress),  $d\varepsilon_p$  is the incremental equivalent plastic strain,  $k$  is the material dependent damageability coefficient which can be determined by monotonic and cyclic material tests in combination of complementary finite element analyses,  $\varepsilon_c$  is the equivalent plastic strain at any load reversal point determined by a switch from a negative to positive triaxiality and  $\eta_{monotonic}$  is the void growth capacity in monotonic tensile loading. In Eq. (3), the monotonic void growth capacity for steel base metal and weld metal is selected to be  $\eta_{monotonic} = 2.5$  and  $2.63$ , respectively and the material dependent damageability coefficient equal to  $k = 0.15$  is used for both materials (Zhou *et al.* 2012).

## 4. Results

### 4.1 Effect of OCR

The corner radii of web openings can have a significant effect on stress and strain concentrations around the opening. According to ASCE 23-97 (1997), the corners of opening should have minimum radii at least 2 times the thickness of the web ( $2t_w$ ), or 16 mm, whichever is greater. This limitation on the corner radii of the opening is based on research by Frost and Leffler (1971), which indicates that corner radii meeting this requirement will not adversely affect the fatigue capacity of a member. In order to study effect of opening corner radii on cyclic behaviour of RWBS connections, the reference model is considered with a rectangular web opening of  $\beta = 0.5$ ,  $\gamma = 1.0$  and different corner radii (Fig. 5).

Fig. 6 displays state of CVGM fracture index at 0.04 rad drift angle for three models along with their hysteresis curves. The curves are presented in black prior to fracture initiation ( $FI_{cyclic} > 1.0$ ),

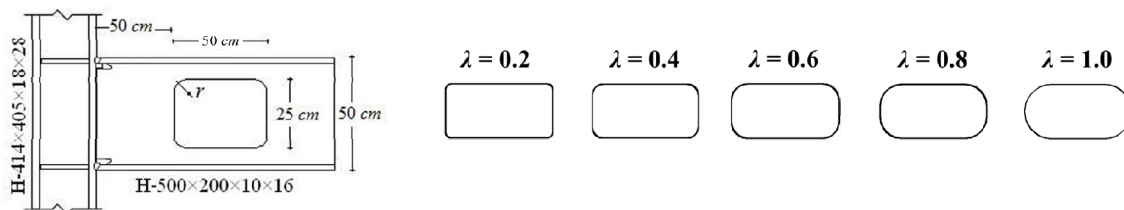


Fig. 5 Configuration of analysed models for evaluating the effect of OCR

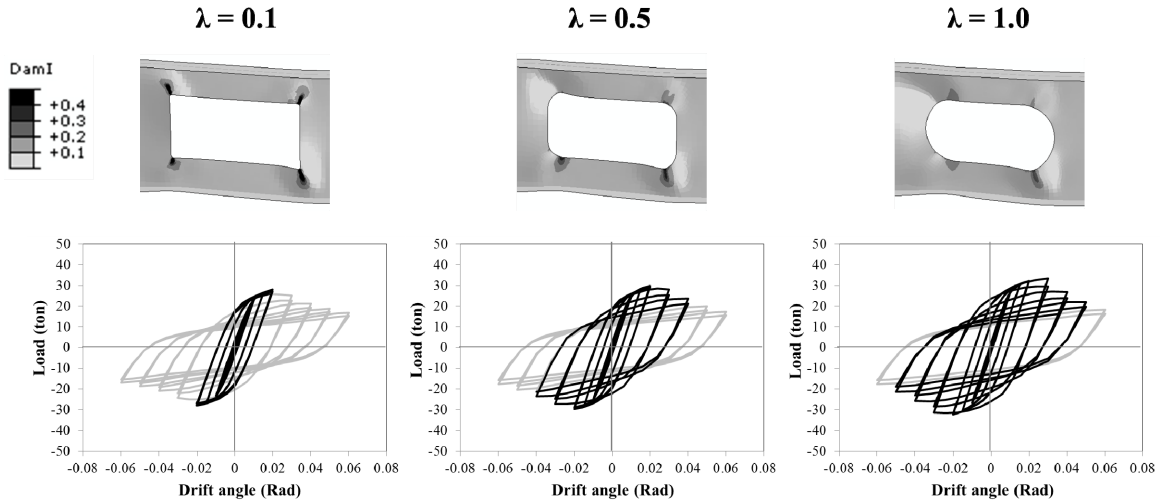


Fig. 6 Effect of OCR on cyclic behaviour of RWBS connections

Table 2 Effect of OCR on the key parameters of cyclic behaviour

No.	$\lambda$	$K_e$ (ton/cm)	$\theta_y$ (rad)	$K_p$ (ton/cm)	$\theta_m$ (rad)	$K_d$ (ton/cm)	$\theta_r$ (rad)	Maximum capacity (ton)	Dissipated energy (kJ)
1	0.1	10.18	0.01	1.87	0.02	1.08	0.01	26.9	77
2	0.2	10.29	0.01	1.88	0.02	1.10	0.02	28.4	149
3	0.3	10.40	0.01	1.86	0.02	1.02	0.03	28.8	173
4	0.4	10.51	0.01	1.89	0.02	1.02	0.03	29.3	200
5	0.5	10.61	0.01	1.93	0.02	1.21	0.03	29.8	244
6	0.6	10.71	0.01	2.00	0.02	1.26	0.04	30.4	274
7	0.7	10.81	0.01	2.05	0.02	1.30	0.04	30.9	320
8	0.8	10.90	0.01	2.09	0.02	1.32	0.04	31.4	307
9	0.9	10.99	0.01	1.53	0.024	1.49	0.04	31.8	364
10	1.0	11.07	0.01	1.30	0.03	1.93	0.05	33.3	398

whereas after fracture initiation they are plotted in gray. Results for other models are summarized in Table 2. According to this figure, after local web buckling takes place the strength, the stiffness, the hysteresis energy, and the load carrying capacity of all specimens deteriorated. For openings with small corner radii the fracture index at corners will be very high. This is in accordance with recommendation of ASCE 23-97 (1997) which indicates that these configurations should not be used in real practice. However, it should be noticed that if it is intended to achieve high rotation capacity at RWBS connections, ASCE 23-97 (1997) requirement about minimum corner radii may be still non-conservative. This can be deduced from the 8th column of Table 2 which indicates that as the opening corner radii increase, the connection rotation capacity increases too.

This is because as the opening corner radii increase the stress and strain concentration and as a result the fracture index at opening corners decreases and hence the connection can undergo higher

rotation capacities. It is worth mentioning that this will be true only if the weakening area is capable of preventing welds from failure and fracture occurs at opening corners. Elastic stiffness of analysed models is presented in the third column of Table 2, from which it can be drawn that the elastic stiffness of the connection will increase as the openings corner radii increase. This increase from the model with  $\lambda=0.1$  to the model with  $\lambda=1.0$  is about 9%. By comparing effective post-yield stiffness,  $K_p$ , rotation angel at maximum strength,  $\theta_m$ , and effective stiffness at degrading segment,  $K_d$ , for different models, it appears that as the opening corner radii increase the loops stabilize at larger amplitudes, but as the possibility of local web buckling at larger deformations is higher, once it occurs the resistance deteriorates more rapidly approaching zero. Two last columns of Table 2 displays effect of corner radii on maximum load carrying capacity and dissipated energy during the cyclic loading. As a result, it can be said that when weakening area is effective in preventing weld fracture, the greater opening corner radii will result in a greater load carrying capacity and dissipated energy of the model.

In general, it can be said that elongated circular holes perform better than rectangular openings with small corner radii. This improved performance is due to the reduced stress concentrations in the region of the opening and the relatively larger web regions in the tees that are available to carry shear. Based on the results of this part, web openings with the maximum possible corner radii ( $\lambda=1.0$ ) will be used for further investigation.

#### 4.2 Effect of opening height and length

The opening length and height are the main design parameters for RWBS connections. Any change in these parameters can affect entire cyclic behaviour of connection. Figs. 7 and 8 summarize configuration of analyzed models and key parameters of hysteresis curves. Graphs of the first row display stiffness and dissipated energy of different models. From Fig. 8(a), it is clear that as the opening height or length increases the initial stiffness of the model decreases. The value of decrease in elastic stiffness from the connection with smallest hole to the model with greatest perforation is about 25%. Figs. 8(b) and (c) display post-yield and degrading stiffness of the models. The general trend for  $K_p$  and  $K_d$  is upwards and downwards respectively, which is a sign of decreasing drift angel associated with the maximum strength,  $\theta_m$ . Accumulated dissipated energy of each model is plotted in Fig. 8(d). As it is clear from this figure, for each height factor there is a unique length factor associated with the maximum dissipated energy (referred to as optimum opening). Connections associated with these points exhibit stable and large hysteresis loops even though some local web buckling at the opening corners is evident after 0.03 rad drift angle. Strength and stiffness of these models remain stable through reasonable inelastic deformations, avoiding the potentially brittle failure in the connection welds. The value of

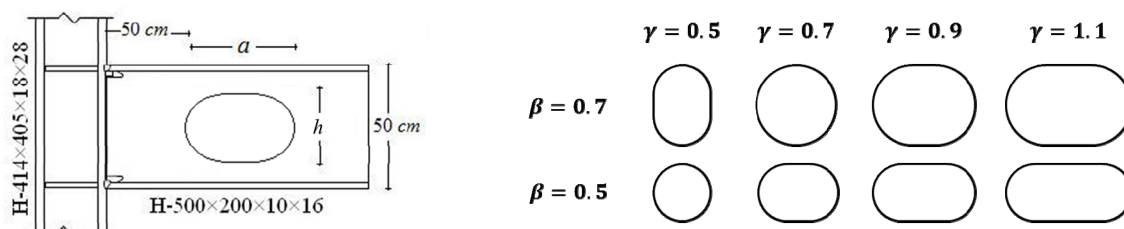


Fig. 7 Configuration of analysed models for evaluating the effect opening height and length

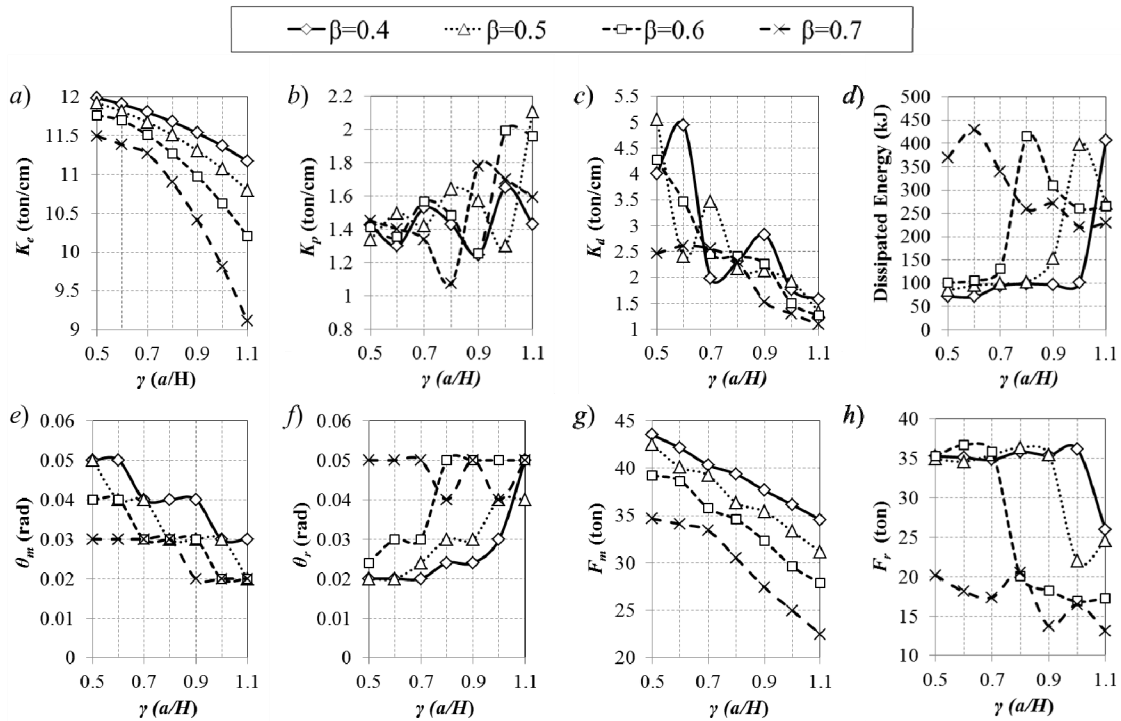


Fig. 8 Effect of opening height and length on the key parameters of cyclic behaviour

decrease in elastic stiffness of these optimum models with respect to the solid model is 6%-8% which seems to be acceptable.

Figs. 8(e) and (f) display drift angles associated with the maximum and residual load carrying capacities. In these graphs, when  $\theta_r$  is less than  $\theta_m$ , the associated model cannot reach its full capacity and fracture at connection welds occurs before connection drift angle can reach  $\theta_m$ . As it can be seen from these graphs, for connections with small opening height or length the failure occurs at connection welds. Also it is shown that as the opening size increases,  $\theta_m$  decreases and  $\theta_r$  increases which is a sign of increased ductility. The value of  $\theta_m$  and  $\theta_r$  for optimum models is 0.03 and 0.05, respectively. The maximum load carrying capacity of analysed models is given in Fig. 8(g) from which the effect opening height and length on reduction of connection strength can be seen. From this figure, the value of decrease in maximum load carrying capacity of optimum models can be determined as 20%. But as in the case solid model or RWBS connections with small opening the connection welds are critical and failure occurs before connection drift angle can reach  $\theta_m$ , maximum load carried by these models will be limited to  $F_r$  which is plotted in Fig. 8(h). Comparing Figs. 8(g) and (h) it can be inferred that the decrease in maximum load carrying capacity of optimum models is less than 5%.

Previous studies indicate that the time of beam web buckling plays a significant role on the total connection strength, such that, an RWBS connection gains most of its strength at this time and after the web buckling the increase in connection strength is not remarkable (Hedayat and Celikag 2009). To prevent elastic buckling of the web, ASCE 23-97 (1997) recommends that the opening parameter,  $p_0$ , should be limited to a maximum value of 5.6 for steel sections

$$p_0 = \frac{a_0}{h_0} + \frac{6h_0}{H} \tag{4}$$

In which  $a_0$  and  $h_0$  are length and width of opening, respectively. This criterion is based on the work of Redwood and Uenoya [19] and is presented for rectangular openings. According to ASCE 23 (1997) this equation can be used for circular openings, substituting  $a_0$  and  $h_0$  by  $0.45D_0$  and  $0.9D_0$ , respectively (where  $D_0$  is diameter of circular opening). Accordingly, for elongated circular holes it can be used making the following substitutions

$$h_0 = [\beta - 0.1 \times \min(\beta, \gamma)] \times H \tag{5}$$

$$a_0 = [\gamma - 0.55 \times \min(\beta, \gamma)] \times H \tag{6}$$

Fig. 9 displays effect of opening depth and length on local buckling of web at the edge of opening. It is worth mentioning that all models of Fig. 9 meet the requirement in Eq. (4). Although, local web buckling occurs in all of these models, it happens after the member yields which is in accordance with the basis of Eq. (4). According to Fig. 9(a), as the length of opening increases, the severity of local web buckling increases, too. Effect of opening depth can be seen in Fig. 9(b). Values reported in this figure are the loading cycles in which the maximum out-of-plane displacement at the edge of opening equals 1/10 of the web thickness. It can be seen from this figure that in most of the cases increasing the opening size decreases the time in which the local web buckling initiates. This is mainly caused by increasing stress level at the corners of opening.

Fig. 10 displays strength of different models with respect to the opening parameter. According to this figure, as the opening parameter decreases the connection strength increases, which is directly caused by delayed local web buckling. As it is shown in this figure, the critical opening parameter,  $P_0 = 4.2$ , separates connections with small opening from connections with large openings. When opening size is small ( $P_0 < 4.2$ ), the weakening area cannot prevent welds fracture and connection fails before reaching its full capacity. On the other hand, when perforation size is large ( $4.2 < P_0 < 5.6$ ) the connection welds is safe but happening of local web buckling reduces

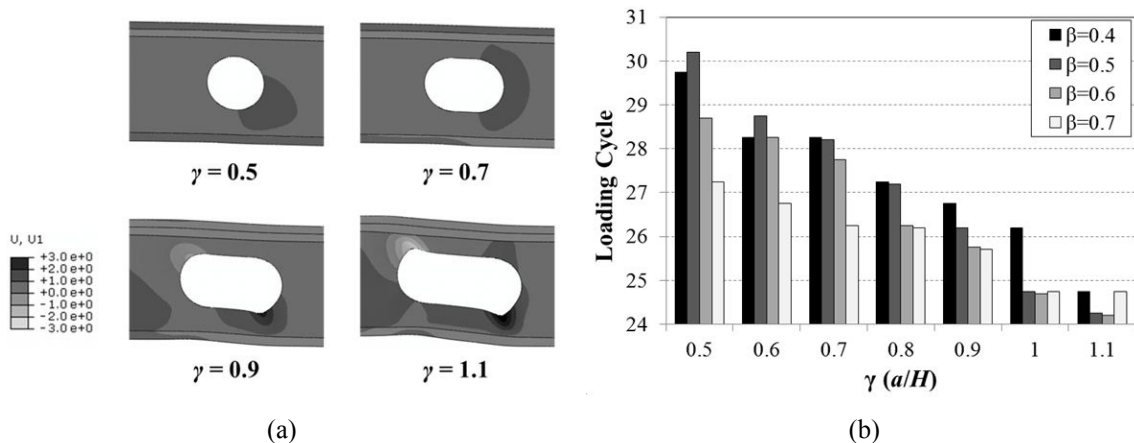


Fig. 9 Effect of opening size on local web buckling: (a) local buckling of web at the edge of opening ( $\beta = 0.5, \theta = 0.03$  rad); (b) local buckling time

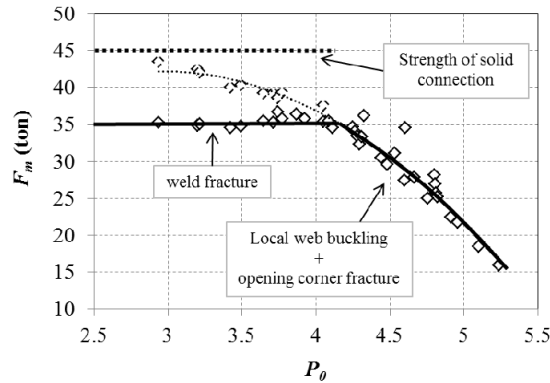


Fig. 10 Effect of opening parameter,  $P_0$ , on connection strength

connection strength. The value of opening parameter for optimum configurations lies almost on the critical opening parameter.

### 4.3 Effect of beam web thickness

Beam web thickness is a key parameter affecting the time in which the local web buckling initiates. From the theoretical point of view it can be expected that the beams with thicker web will be able to undergo larger deformations prior to local web buckling. Since RWBS connections gain most of their strength before local web buckling, any change in beam web thickness will affect cyclic behaviour of these connections. To see effect of web thickness on the cyclic behaviour of RWBS connections, the numerical models are reanalysed using two different values for beam web thickness in addition to the original value. The resultant parameters of idealized backbone curve for one of models with optimum opening dimensions ( $\beta = 0.6, \lambda = 1.0$ ), are summarized Table 3. The general trend for other models is almost the same.

Comparing the stiffness of different models it can be inferred that as the beam web thickness increases, the elastic stiffness of connection increases too. Decrease of  $K_p$  and increase of  $K_d$  with respect to increasing web thickness are the sign of delayed local web buckling accompanied by a steeper post capping degradation. Comparing the rotation angle corresponding to maximum load carrying capacity,  $\theta_m$ , it is apparent that as the beam web thickness increases the local web buckling occurs at higher deformations. It is worthy to note that as the web thickness increases to 1.2 cm, the premature failure occurs at connection welds and model cannot reach its maximum capacity ( $\theta_r < \theta_m$ ).

Table 3 Effect of beam web thickness on the key parameters of cyclic behaviour ( $\beta = 0.6, \lambda = 1.0$ )

No.	Beam web thickness (cm)	Stiffness (ton/cm)			Rotation angle (rad)		Load carrying capacity (ton)		Dissipated energy (kJ)
		$K_e$	$K_p$	$K_d$	$\theta_m$	$\theta_r$	$F_{max}$	$F_r$	
1	0.8	10.71	2.51	1.62	0.015	0.05	28.39	12.49	257
2	1.0	11.27	1.48	2.41	0.03	0.05	34.59	20.07	415
10	1.2	11.73	1.35	3.03	0.04	0.03	38.64	36.64	134

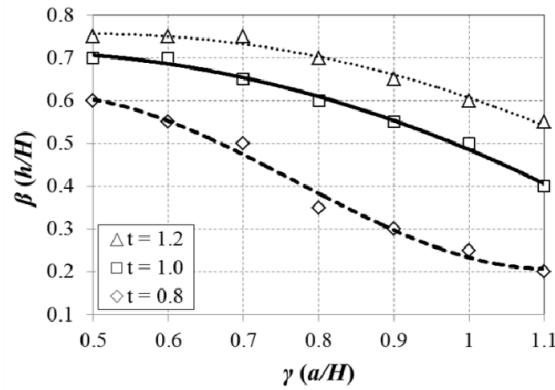


Fig. 11 Effect of web thickness on the optimum opening height and length

The last column of this table displays effect of beam web thickness on the accumulated dissipated energy of RWBS connections. As a conclusion, any change in beam web thickness of a connection with optimum web opening will decrease dissipated energy of the model. For beams with thinner and thicker webs further decrease in load carrying capacity and premature failure at connection welds are responsible for decreased energy dissipation, respectively. Fig. 11 displays effect of beam web thickness on the optimum combination of opening height and length. Compared with the original curve it can be inferred that as the beam web thickness increases, the required opening size to have a connection with maximum energy dissipation increases, too.

Fig. 12 displays pushover behaviors obtained from cyclic load-displacement curves for the last three connections with optimum opening dimensions of Fig. 11 (models with  $\gamma = 1.1$ ). From these curves, it can be inferred that as the beam web thickness increases local buckling of web occurs at higher rotation angles. For models with  $t = 0.8$ , 1.0 and 1.2, local web buckling initiates at  $\theta = 0.02$ , 0.03 and 0.04, respectively. It is interesting to note that, although beams with thinner web have lower load carrying capacity, their strength deterioration after local buckling is more slowly. On the other hand, beams with thicker web have higher energy absorption and more stable hysteresis loops.

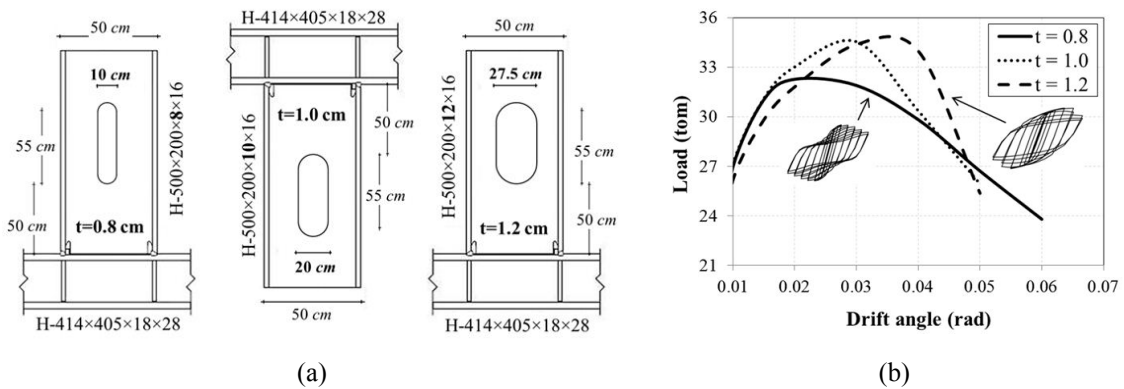


Fig. 12 Effect of web thickness on pushover behavior: (a) configuration of models; (b) pushover curves

#### 4.4 Effect of opening stiffeners

An effective method of eliminating the detrimental effects of a large web opening is to attach suitable stiffeners around the web openings. Such stiffeners are used to reduce the local buckling effects of free edges. As the strength of RWBS connections is mainly governed by local web buckling, these stiffeners are likely to have a great effect on the ultimate shear strength of connection. To see effect of opening stiffeners on the cyclic behaviour of RWBS connections, a set of models with stiffened openings are analysed and compared to connections with unreinforced web openings. Stiffeners are placed at the edge of opening and assumed to be continuous on entire perimeter of the web opening. The thickness of stiffeners is assumed to be equal to the beam web thickness, 10 mm, while their height is 20 mm on both sides of the web. It should be noted that these dimensions are not the optimum values for opening stiffener and evaluation of optimum stiffening for web opening needs more study, but comparing results of models with these stiffeners to those with unstiffened openings may be useful. Effect of opening stiffener on local buckling of RWBS connections under cyclic loading is displayed in Fig. 13. In both models, the opening height and width factors are 0.4 and 1.0, respectively. As it can be seen in the figure, addition of opening stiffener causes the change of “local web buckling mode” to “local flange buckling mode”. However it should be noted that local buckling of flange usually occurs in higher drift angles compared to the local web buckling.

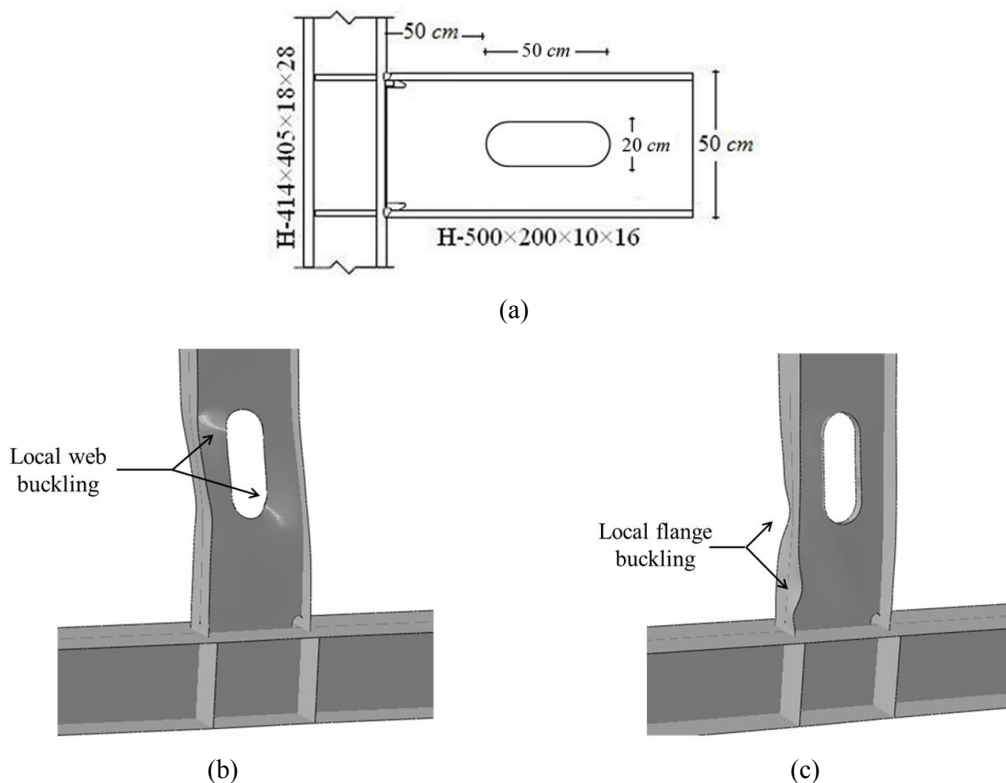


Fig. 13 Effect of opening stiffener on local buckling of beam: (a) configuration of analysed model; (b) opening without stiffener; (c) opening with stiffener

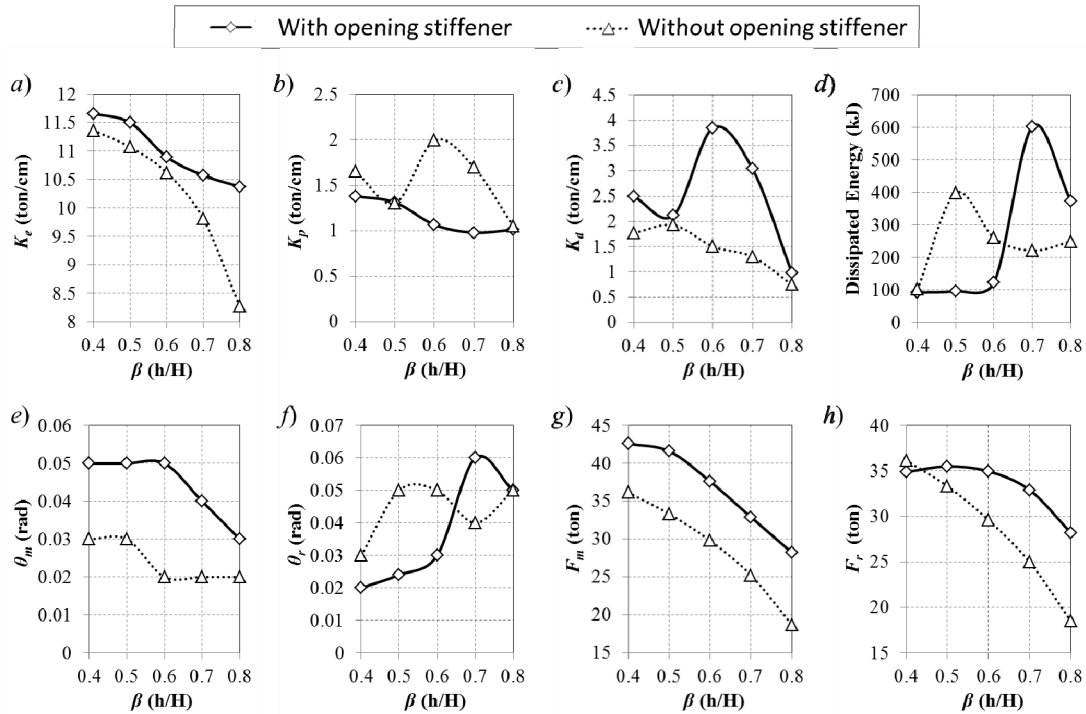


Fig. 14 Effect of opening stiffener on the key parameters of cyclic behaviour

To have a closer look at the issue, a set of RWBS connections with a fixed width of  $\gamma = 1.0$  and varying height factors are analysed with and without opening stiffeners. The key parameters of hysteresis curve for both models are compared in Fig. 14. According to the first graph, for both models the initial stiffness of the connection decreases with the increase of opening height. However, the decrease of stiffness in models with unstiffened opening edge is more evident. The second and third graphs display post-yield stiffness and degrading slope of the hysteresis curves. As it can be seen, models with stiffened openings have a lower post-yield stiffness which can be caused by a greater inelastic plateau of these models. It is also displayed that strength deterioration is comparatively rapid in reinforced opening case. Cumulative dissipated energy of analysed models is plotted in the fourth graph, from which one can deduce that for models with stiffened opening the maximum energy dissipation can be achieved using a greater perforation size. Also it can be seen that the value of maximum dissipated energy for the model with opening stiffener is higher compared to the unreinforced opening case which can be a sign of increased ductility of connection.

Graphs of the lower row display maximum and residual strengths and associated deformations. Same as Fig. 9, when  $\theta_r$  is less than  $\theta_m$ , fracture occurs at connection welds. Accordingly, in the case of stiffened openings, when opening size is small the connection welds will be critical. For these models, although connection is capable of reaching a maximum load of  $F_m$ , in reality the maximum load carried by connection will be limited to  $F_r$ . However it is evident from graphs that models with stiffened opening edge have higher strength and deformation capacity which is mainly caused by decreased potential of connection to local web buckling and increased plastic capacity of tee-sections above and below the opening area.

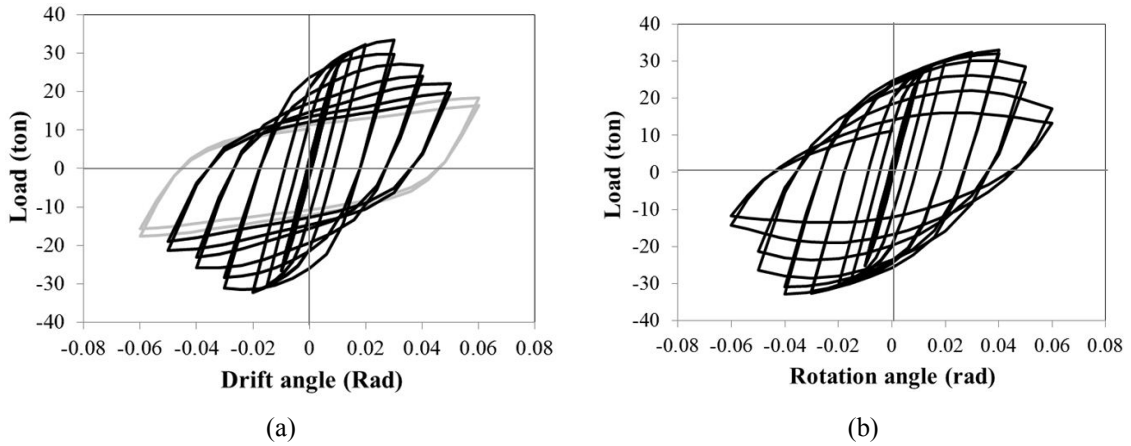


Fig. 15 Comparison of hysteresis curves for optimum openings with and without stiffeners

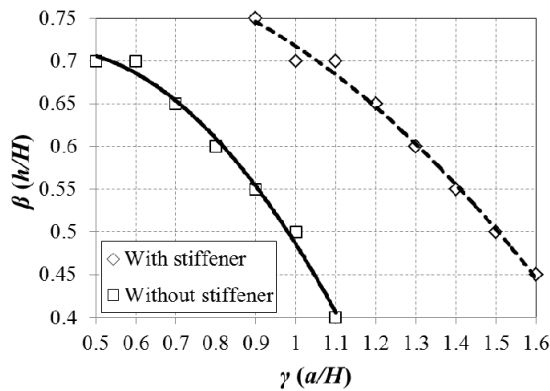


Fig. 16 Effect of opening stiffener on the optimum opening height and length

This improved behaviour of stiffened openings can be seen in Fig. 15 which compares the hysteresis curves for optimum openings with and without stiffeners. According to this figure, although both connections have acceptable hysteresis curves, the one with opening stiffeners appears to be more stable and ductile. Cyclic behaviour of these models can be compared to those with stocky web. However, as it may be economical to add perimeter stiffener at the edge of opening rather than using a beam with thicker web, the connections with stiffened openings may be preferred. By conducting numerical analysis on models with stiffened openings of varying width, the optimum opening height and length are obtained for these connections and plotted in Fig. 16. According to this figure, a greater perforation size is needed for stiffened openings to achieve maximum deformation capacity and energy dissipation.

### 5. Conclusions

In this paper a parametric study is implemented in order to evaluate effect of local web buckling on the cyclic behaviour of Reduced Web Beam Sections (RWBS). For this purpose, three

dimensional finite element models of the RWBS connections are established. The failure of specimens under Ultra-Low Cycle Fatigue (ULCF) condition is modeled using Cyclic Void Growth Model (CVGM). Effect of opening corner radii, opening height and length, beam web thickness and opening stiffeners are studied. Based on the results, for openings with small corner radii the fracture index at corners will be very high. This is in accordance with recommendation of ASCE 23-97 (1997) which indicates that these configurations should not be used in real practice. However, it should be noticed that if it is intended to achieve high rotation capacity at RWBS connections, ASCE 23-97 (1997) requirement about minimum corner radii may be still non-conservative. In general, it can be said that elongated circular holes perform better than rectangular openings with small corner radii. Height and length of these openings are the main design parameters which affect cyclic behaviour of connection. Increasing the size of opening causes formation of Vierendeel mechanism in weakened area which in earlier stages can protect connection welds from failure, but care should be taken as further increase in opening height or length expedites initiation of local web buckling and causes significant stiffness and strength degradation. Comparing models with different openings it is concluded that for each opening height factor there is a unique length factor resulting in a model with the maximum dissipated energy. Connections with these optimized perforation sizes exhibit stable and large hysteresis loops.

Evaluation of models with different beam web thickness revealed that, for connections with thicker beam web, local buckling around the opening occurs at higher rotation angles giving them higher energy absorption and more stable hysteresis loops. Also, it is shown that as the beam web thickness increases, the size of optimum openings increases, too. Addition of perimeter stiffener to openings had the same effect as thickening of the beam web except that for these models even a greater opening size is needed to have a connection with maximum energy dissipation.

## References

- ANSI/AISC 341 (2010), Seismic Provisions for Structural Steel Buildings; American Institute of Steel Construction, Chicago, IL, USA.
- ASCE 23-97 (1997), Proposed specification for structural steel beams with web opening; American Society of Civil Engineers (ASCE).
- Chung, K.F., Liu, T.C.H. and Ko, A.C.H. (2001), "Investigation on Vierendeel mechanism in steel beams with circular web openings", *J. Construct. Steel Res.*, **57**(5), 467-490.
- Darwin, D. (2000), "Design of composite beams with web openings", *Progress Struct. Eng. Mater.*, **2**(2), 157-163.
- Erfani, S., Babazadeh Naseri, A. and Akrami, V. (2012), "The beneficial effects of beam web opening in seismic behavior of steel moment frames", *Steel Compos. Struct., Int. J.*, **13**(1), 35-46.
- Frost, R.W. and Leffler, R.E. (1971), "Fatigue tests of beams with rectangular web holes", *ASCE J. Struct. Div.*, **97**(2), 509-527.
- Hancock, J.W. and Mackenzie A.C. (1976), "On the mechanisms of ductile failure in high-strength steel subjected to multi-axial stress-states", *J. Mech. Phys. Solid.*, **24**(2-3), 147-160.
- Hedayat, A.A. and Celikag, M. (2009), "Post-Northridge connection with modified beam end configuration to enhance strength and ductility", *J. Construct. Steel Res.*, **65**(7), 1413-1430.
- Kanvinde, A.M. and Deierlein G.G. (2004), "Micromechanical simulation of earthquake induced fracture in steel structures", Report No. 145; Blume Earthquake Engineering Center, Stanford University, Stanford, CA, USA.
- Kazemi, M.T. and Erfani, S. (2007), "Analytical study of special girder moment frames using a mixed shear-flexural link element", *Can. J. Civil Eng.*, **34**(9), 1119-1130.

- Kazemi, M.T., Momenzadeh, S.B. and Hoseinzadeh Asl, M. (2012), "Study of reduced beam section connections with web opening", *Proceedings of the 15th World Conference on Earthquake Engineering (15WCEE)*, Lisbon, Portugal, September.
- Lee, E.T., Chang, K.H., Shim, H.J. and Kim, J.H. (2004), "Local buckling behavior of steel members with web opening under cyclic loading", *Proceedings of the 7th Pacific Structural Steel Conference (7PSSC)*, Long Beach, CA, USA, March.
- Lepage, A., Aschheim, M. and Senescu, R. (2004), "Shear-yielding steel outriggers for high-rise construction", *Proceedings of the 13th World Conference on Earthquake Engineering (13WCEE)*, Vancouver, Canada, August.
- Liu, T.C.H. and Chung, K.F. (2003), "Steel beams with large web openings of various shapes and sizes: finite element investigation", *J. Construct. Steel Res.*, **59**(9), 1159-1176.
- Myers, A.T., Deierlein, G.G. and Kanvindeh, A. (2009), "Testing and probabilistic simulation of ductile fracture initiation in structural steel components and weldments", Report No. 170; Blume Earthquake Engineering Center, Stanford University, Stanford, CA, USA.
- Redwood, R.G. and Cho, S.H. (1993), "Design of steel and composite beams with web openings", *J. Construct. Steel Res.*, **25**(1-2), 23-41.
- Redwood, R.G. and Uenoya, M. (1979), "Critical loads for webs with holes", *ASCE J. Struct. Div.*, **105**(10), 2053-2067.
- Rice, J.R. and Tracey, D.M. (1969), "On the ductile enlargement of voids in triaxial stress fields", *J. Mech. Phys. Solid.*, **17**(3), 201-217.
- Shinde, H., Kurobane, Y., Azuma, K. and Dale, K. (2003), "Additional full-scale testing of beam-to-column connections with improvements in welded joints", *Proceedings of the 13th International Offshore and Polar Engineering Conference*, Honolulu, HI, USA, May.
- Tsavdaridis, K.D. and D'Mello, C. (2012), "Optimisation of novel elliptically-based web opening shapes of perforated steel beams", *J. Construct. Steel Res.*, **76**, 39-53.
- Yang, Q., Li, B. and Yang, N. (2009), "Aseismic behaviors of steel moment resisting frames with opening in beam web", *J. Construct. Steel Res.*, **65**(6), 1323-1336.
- Zhou, H., Wanga, Y., Shi, Y., Xiong, J. and Yang, L. (2012), "Extremely low cycle fatigue prediction of steel beam-to-column connection by using a micro-mechanics based fracture model", *Int. J. Fatigue*, **48**, 90-100.